Low-energy electron scattering from halomethanes. III. e-CF_3Cl

1992 J. Phys. B: At. Mol. Opt. Phys. 25 1621

(http://iopscience.iop.org/0953-4075/25/7/030)

J. Phys. B: At. Mol. Opt. Phys. **25** (1992) 1621-1632. Printed in the UK

Low-energy electron scattering from halomethanes: III. e–CF_3Cl*

A Mann and F Linder

Fachbereich Physik, Universität Kaiserslautern, W-6750 Kaiserslautern, Federal Republic of Germany

Received 24 July 1991, in final form 5 December 1991

Abstract. Differential cross sections for elastic scattering and vibrational excitation in low-energy (0.5-10 eV) e-CF_3Cl collisions have been measured. The integral elastic and the total inelastic cross section are determined. In the domain of resonance-enhanced vibrational excitation, the C-Cl and C-F stretching modes are predominantly excited according to the character and the symmetry type of the respective resonance. The strongest excitation is observed for the symmetric C-Cl stretching mode in the energy region of the A_1 (C-Cl σ^*) resonance at 2.0 eV. The E (C-F σ^*) and A_1 (C-F σ^*) resonances have been assigned for the first time; they are found to be located at 5.5 eV and 8.5 eV, respectively, and lead to predominant excitation of CF_3 stretching modes. More details of the observed mode-selective excitation are discussed in the paper. The excitation of the IR-active modes is compared with the Born dipole approximation. The relation with dissociative attachment results is briefly discussed.

1. Introduction

The interaction of low-energy electrons with CF_3Cl contains several aspects of interest. The first to mention is related to the series $CF_{4-n}Cl_n$ and concerns the changes in the scattering behaviour which appear upon the substitution of the halogen atoms. In contrast to e-CF_4 with its rather flat cross section at low energies, the e-CF_3Cl scattering shows a clearly peaked resonance around 2 eV (Jones 1986) which is most probably associated with the occupation of the A_1 (C-Cl σ^*) valence type orbital. The substituted Cl atom leads to a lower symmetry of the molecule (point group C_{3v}) and thus to a lower degeneracy of the electronic orbitals and vibrational modes. The three (C-F σ^*) valence orbitals group into two resonances of A_1 (C-F σ^*) and E (C-F σ^*) type which have not yet been assigned to definite energy values. The number of non-degenerate normal modes increases from four to six, and one has to expect a more complex pattern of vibrational excitation. Nevertheless, the excitation of stretching modes should still be dominant according to the localization of the σ^* resonance orbitals along the C-F and C-Cl axis, respectively.

Another aspect is given by the importance of electron–halocarbon interaction processes in several applications such as plasma etching or gaseous dielectrics (Christophorou and Hunter 1984). In this context, the determination of absolute cross sections for the different processes is especially desirable. To our knowledge, no results exist on elastic scattering or vibrational excitation, while electron attachment has been

* This work represents part of the doctoral thesis of A Mann.

0953-4075/92/071621+12$04.50

studied in several papers (Schumacher *et al* 1978, Illenberger 1982, Spyrou and Christophorou 1985). Absolute values are known for the total electron scattering cross section (Jones 1986) and for total electron attachment (Spyrou and Christophorou 1985). Verhaart *et al* (1978) have reported experiments on electron transmission, dissociative attachment, and threshold electron-impact excitation. They propose Rydberg-type resonances for e-CF_3Cl and e-CF_4 scattering in the 0-2 eV region which are questioned, however, by more recent experiments of Jordan and Burrow (1987). The observed structures are probably due to the strong excitation of the IR-active modes at their respective thresholds.

In this paper, we present the results of our differential scattering experiments for the system e-CF_3Cl. They cover the collision energy range from 0.5 to 10 eV and detection angles from 10° to 105°. For a description of the apparatus and the experimental method we refer to the preceding papers I and II (Mann and Linder 1992a, b).

2. Elastic scattering

The DCS for elastic e-CF_3Cl scattering has been measured by either scanning the collision energy or the detection angle. The results are presented in figures 1 and 2 and in table 1. Remarkable features are the small cross sections for collision energies below 1 eV and the general increase of the cross section for small scattering angles. The position of the low-energy minimum shifts to lower energies for growing angles and thus shows the typical energy dependence of the Ramsauer-Townsend effect. The minimum is less pronounced than in the case of CF_4 which is probably due to a larger contribution of partial waves with $l > 0$ as well as considerable rotational excitation, both caused by the permanent dipole moment of CF_3Cl (0.5 D). We refer to Itikawa

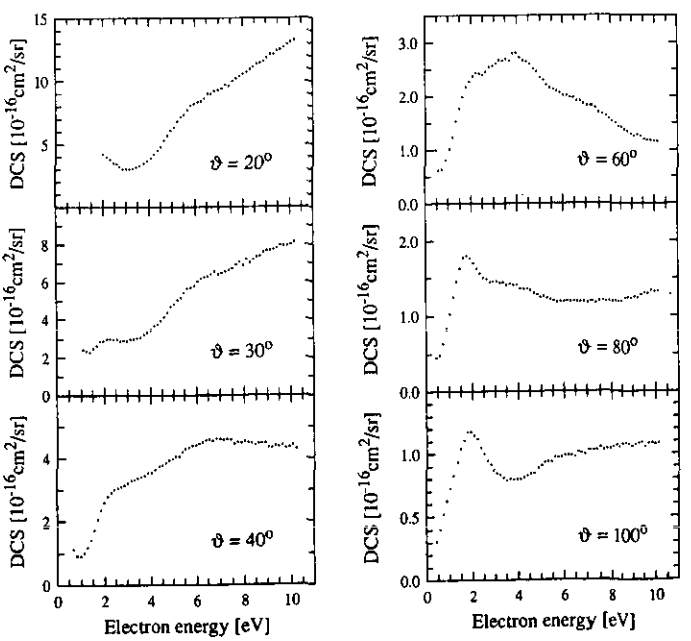

Figure 1. Energy spectra for elastic e-CF_3Cl scattering at different scattering angles.

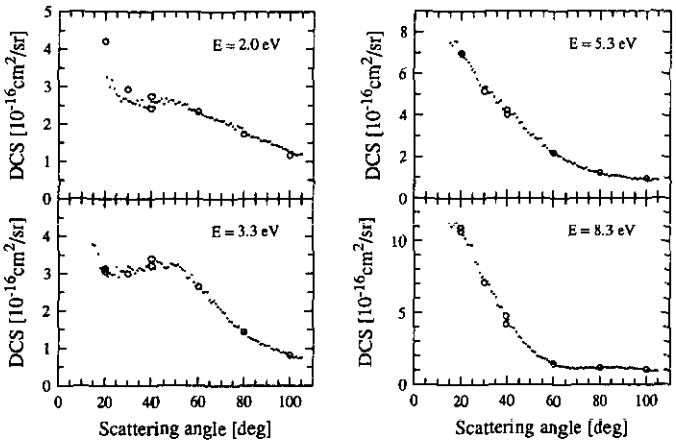

Figure 2. Angular spectra for elastic e-CF_3Cl scattering at different collision energies. The open circles are derived from the measured energy spectra (see figure 1).

Table 1. Differential cross section $d\sigma/d\Omega$ (10^{-16} cm^2 sr^{-1}) for elastic e-CF_3Cl scattering. The experimental errors are estimated to about 20–30% and up to 40% for small energies and angles.

	Scattering angle (deg)					
Energy (eV)	20	30	40	60	80	100
0.5	—	—	—	0.81	0.45	0.34
1.0	—	2.42	0.95	0.95	0.98	0.70
1.5	—	2.46	1.61	1.81	1.65	1.05
2.0	4.21	2.93	2.58	2.33	1.74	1.16
2.5	3.47	2.97	3.02	2.44	1.52	1.00
3.0	3.03	2.92	3.19	2.58	1.45	0.86
3.5	3.19	3.08	3.37	2.68	1.43	0.80
4.0	3.83	3.45	3.54	2.76	1.39	0.79
4.5	4.89	3.98	3.78	2.60	1.34	0.83
5.0	6.24	4.74	4.00	2.35	1.26	0.90
5.5	7.40	5.39	4.25	2.14	1.21	0.95
6.0	8.24	5.93	4.43	2.03	1.19	0.98
6.5	8.83	6.31	4.57	1.95	1.19	0.99
7.0	9.33	6.46	4.61	1.85	1.18	1.02
7.5	9.88	6.71	4.53	1.71	1.19	1.04
8.0	10.56	7.00	4.50	1.56	1.19	1.05
8.5	11.22	7.24	4.46	1.41	1.20	1.07
9.0	11.81	7.63	4.40	1.29	1.24	1.07
9.5	12.42	7.85	4.38	1.21	1.29	1.08
10.0	13.02	8.01	4.36	1.16	1.33	1.08

(1971) for a theoretical treatment of rotational excitation of symmetric top molecules in terms of the Born approximation.

At $E = 2$ eV, all energy spectra show a structure, either a peak or a shoulder, which is easily attributed to the A_1 (C-Cl σ^*) resonance at this energy (Jones 1986). No common features appear above that energy, and different trends are observed for different scattering angles. Below $\vartheta \sim 40°$, the cross section starts to increase with the

collision energy and reaches 1.3×10^{-15} cm^2 sr^{-1} for $E = 10$ eV and $\vartheta = 20°$. This value is more than 10 times larger than the average cross section at $\vartheta = 100°$.

The angular spectra (figure 2) are taken at four collision energies which have been selected according to the shape of the total cross section (Jones 1986, see figure 3). The values 2.0, 5.3, and 8.3 eV are approximately related to maxima and thus probably to resonances, while at 3.3 eV a deep minimum is observed and one may expect non-resonant scattering. As a general trend, all angular spectra show a decreasing cross section with growing scattering angle. For $E = 2.0$ eV and 3.3 eV, a step-like structure appears between 25° and 50°. At the higher energies, we observe a monotonic decrease down to $\sim 10^{-16}$ cm^2 sr^{-1} with an additional local maximum around 90° for $E = 8.3$ eV.

As in paper I on CF_4, the integral cross section for elastic scattering is obtained by extrapolation, and the difference to the total cross section of Jones (1986) gives the total inelastic cross section. These curves are depicted in figure 3 together with the Born dipole approximation for the total vibrational excitation cross section (BDA, Itikawa 1974a). The dipole moments are taken from Bishop and Cheung (1982) and listed in table 2. The absolute cross section values of the present work are again determined with reference to the work of Jones (1986) similar to the procedure described in paper I. The sum of elastic scattering and vibrational excitation in the resonance-free region around 3.0–3.5 eV is normalized to the measured total cross section. Dissociative attachment is negligible at this energy (Illenberger 1982).

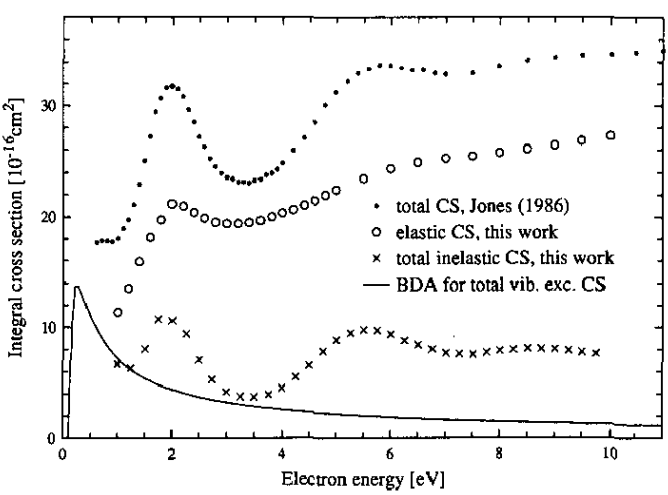

Figure 3. Comparison of various integral cross sections for e-CF_3Cl scattering. The total inelastic cross section is obtained as the difference between the total cross section (Jones 1986) and our integral elastic cross section. Also shown is the Born dipole approximation (BDA) for the total vibrational excitation cross section (sum of ν_1, ν_2, ν_4, ν_5).

While the two lowest resonances at 2.0 eV and at 5.5–6.0 eV are clearly visible in the total and in the total inelastic cross section, the corresponding structures are much less pronounced in the integral elastic cross section. The weak structure in the inelastic cross section around 8.5 eV can also be connected with an electron capture process. The resonances will be discussed in more detail in the following paragraphs together with the results for the various decay channels.

3. Vibrational excitation

A first survey of vibrational excitation in e-CF_3Cl scattering is given by the energy loss spectra shown in figure 4. The collision energies are similar to those in figure 2 and are representative of different scattering regimes. Due to the six normal modes (see table 2), the excitation pattern is somewhat confusing at first sight and quite different in all four spectra. A strong excitation of the stretching modes ν_1 and ν_4 appears in all of them, but the individual contributions of the two modes cannot be determined unambiguously with an experimental energy resolution of $\Delta E \sim 25$ meV (FWHM). Another marked peak appears at $E = 5.5$ eV and $E = 8.2$ eV which corresponds to the excitation of $2\nu_{1,4}$. Again, apparently both modes are excited with a stronger contribution of ν_1 at 5.5 eV and of ν_4 at 8.2 eV. The CF_3 deformation modes ν_2 (1.7 eV, 8.2 eV) and ν_5 (5.5 eV) are also observed. The excitation of the C-Cl stretching mode ν_3 appears only at 1.7 eV, but there it is remarkably strong and even surpasses the $\nu_{1,4}$ excitation. All other assigned energy losses in figure 4 are tentative and the main purpose is to indicate the respective positions in the energy loss spectra.

Regarding the high number of possible energy losses, the excitation schemes are not too complicated. In connection with the selection rules for direct and resonant

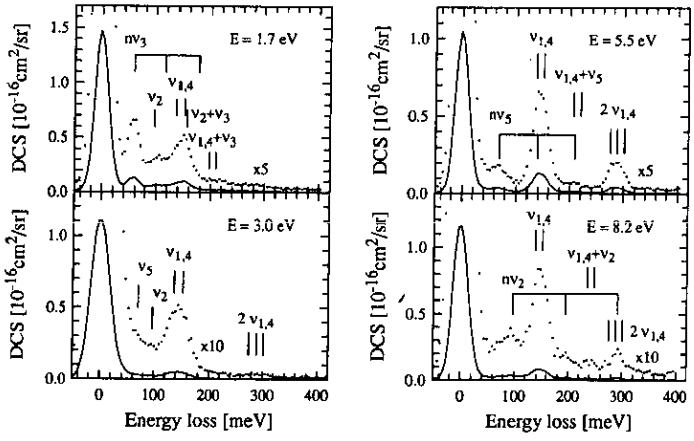

Figure 4. Energy loss spectra for e-CF_3Cl scattering at $\vartheta = 90°$ and different collision energies. The energy losses due to excitation of the various vibrational modes are indicated by vertical bars.

Table 2. Vibrational modes of CF_3Cl (point group C_{3v}, $\Gamma_v = 3A_1 + 3E$) with respective energies, symmetry types and important activities (from Herzberg 1945, Sverdlov *et al* 1974, Scanlon *et al* 1981). The value of the sum of the squared dipole matrix elements M_n^d ($e^2a_0^2$) (see II) is given with the IR-active modes (Bishop and Cheung 1982).

Mode	E (meV)	Nuclear motion	Symmetry	Activity
ν_1	137.4	CF_3 symmetric stretch	A_1	IR (0.0314), Raman (m)
ν_2	97.2	CF_3 symmetric deformation	A_1	IR (0.0028), Raman (s)
ν_3	59.1	C-Cl symmetric stretch	A_1	Raman (s)
ν_4	150.5	CF_3 asymmetric stretch	E	IR (0.0343)
ν_5	69.7	CF_3 asymmetric deformation	E	IR (0.0003)
ν_6	43.2	F_3-C-Cl bending	E	

vibrational excitation (see paper II), they can be traced back to simple principles. Starting with the non-resonant excitation at $E = 3.0$ eV, we can state that only the IR-active modes appear significantly. In the first resonance region at $E = 1.7$ eV, the direct mechanism can probably still account for the observed $\nu_{1,4}$ excitation, although there may be some $\nu_2 + \nu_3$ contribution. Due to the supposed A_1 (C-Cl σ^*) character of this resonance, the symmetric C-Cl stretching mode ν_3 should dominate the energy loss in agreement with the observation. The weakly excited ν_2 belongs to the symmetry type A_1 and thus obeys the selection rules. The CF_3 deformation seems to be compatible with the (C-Cl σ^*) character of the resonance, if one recalls that the charge distribution of the additional electron along the C-Cl axis reaches beyond the carbon atom into the CF_3 part of the molecule. The observed excitation behaviour is thus in agreement with the A_1 (C-Cl σ^*) assignment of the 2 eV resonance.

No assignment has yet been made for the higher resonances which are expected to be of (C-F σ^*) valence type with A_1 and E symmetry. While the C-F stretching modes should dominate in both cases, the selection rules predict exclusive excitation of A_1 modes in the A_1 resonance and excitation of A_1 or E modes in the E resonance. The most striking difference between the energy loss spectra at 5.5 eV and at 8.2 eV is the excitation of ν_5 (E) and ν_2 (A_1), respectively. Hence we conclude that the resonance at 5.5 eV is of symmetry type E, while the resonance around 8.5 eV is assigned to the A_1 species. The excitation of ν_4 at 8.2 eV, which is forbidden in the A_1 resonance by the selection rules, may be attributed to other non-resonant mechanisms which are operative at these higher energies (see also discussion of figure 6).

In figure 5, an energy loss spectrum at $E = 5.5$ eV is shown covering the excitation of overtones up to $n = 6$. The energy shift due to the anharmonicity of the potential is in the order of -1 meV per vibrational quantum (de Souza and Perry 1986). It appears that always both modes are excited with some emphasis on ν_1 at the higher excitations. This spectrum is an example of the high selectivity in electron-impact vibrational excitation under certain conditions. The selective excitation of both ν_1 and ν_4 is in agreement with the assignment of the 5.5 eV resonance as E (C-F σ^*).

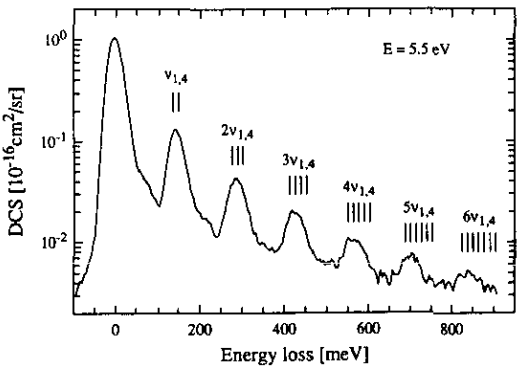

Figure 5. Energy loss spectrum at $E = 5.5$ eV and $\vartheta = 90°$. The indicated energy loss processes $n\nu_{1,4}$ correspond to the multiplet $(n-k)\nu_1 + k\nu_4$, $k = 0, \ldots, n$.

With knowledge of the important energy loss processes, one can look at the respective excitation functions. In figure 6, we present some measured spectra for the excitation of $\nu_{1,4}$, $2\nu_{1,4}$, ν_3, and ν_2 at $\vartheta = 90°$. It has to be kept in mind that a fixed

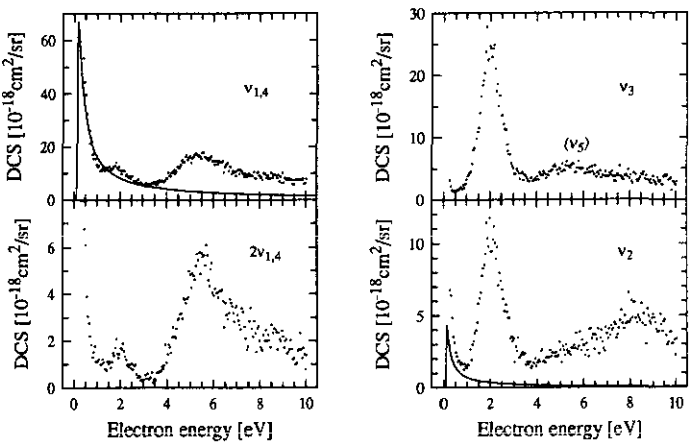

Figure 6. Excitation functions for the most important energy loss processes in e-CF_3Cl scattering at $\vartheta = 90°$. The full lines represent the Born dipole cross section for the excitation of $\nu_{1,4}$ and ν_2. The second maximum in the ν_3 excitation function is probably due to excitation of ν_5 (see text).

energy loss is not always uniquely related to the excitation of one particular mode and an admixture of other contributions may be present depending on scattering energy and angle. In particular, this may be important for the $\nu_{1,4}$ excitation around 2 eV (neighbourhood of $\nu_3+\nu_2$), the ν_3 excitation above ~3 eV (overlap with ν_5), and the ν_2 excitation (tail of ν_3 and $\nu_{1,4}$). However, in the regions of strong excitation the indicated modes are clearly dominating. The position of the resonances and their influence on the excitation of the various modes as discussed before are now directly visible. In addition, it becomes evident that below the 2.0 eV resonance the cross section for IR-active modes is steeply increasing towards low energy. This direct scattering process is compared with the Born dipole approximation which is calculated as described in paper II (referring to Itikawa 1974a). The BDA for $\nu_{1,4}$ is simply the sum of the cross sections for ν_1 and ν_4. The agreement with the measured cross section below 1.5 eV and in the non-resonant region around 3 eV is well within the experimental error bars. The BDA for the weakly IR-active mode ν_2 agrees in shape with the experimental curve, but has only about half the size. If one accepts the tabulated IR absorption value for ν_2, the most probable reason for this difference is the excitation via higher multipole moments and polarization interactions (Itikawa 1974a, b).

The excitation functions allow a further discussion of the influence of the resonances on vibrational excitation. It appears that the $\nu_{1,4}$ excitation at 2 eV is mostly due to non-resonant scattering. This statement is corroborated by the excitation function of $2\nu_{1,4}$ which is quite small at 2.0 eV compared to its value of $\sim 6\times10^{-18}$ cm^2 sr^{-1} at 5.5 eV. At 8.5 eV, where a resonant ν_4 excitation would contradict the selection rules, a considerable $\nu_{1,4}$ and $2\nu_{1,4}$ excitation is observed, but without a pronounced peak at this energy. It appears likely that at this relatively high energy (above the threshold for electronic excitation at ~7.5 eV; Verhaart *et al* 1978) a large portion of the $\nu_{1,4}$ and $2\nu_{1,4}$ excitation is due to direct scattering. On the other hand, a clear peak is obtained in the excitation function of ν_2. In this case, the symmetry type of the vibrational mode is in agreement with the selection rules, and the observed peak in the ν_2 excitation function at 8.5 eV lends strong support to the assignment of the A_1 (C-F σ^*) resonance to this energy.

Over the whole range of collision energies studied, the ν_3 excitation is constrained to a rather narrow region around 2.0 eV. Here, the cross section reaches $\sim 2.5 \times 10^{-17}$ cm^2 sr^{-1}. This value is the largest cross section observed for resonant vibrational excitation of CF_3Cl. The second maximum in the excitation function of ν_3 around 5.5 eV is most probably due to the excitation of ν_5 as suggested by the energy loss spectrum in figure 4 (the difference in energy loss between ν_3 and ν_5 is only 10.6 meV). A similarly large and narrow peak at the 2.0 eV resonance is found in the ν_2 excitation function with a maximum of $\sim 1.1 \times 10^{-17}$ cm^2 sr^{-1}, but here we observe additional resonant excitation at 8.5 eV and a contribution of direct excitation below 0.5 eV.

In figure 7, we present the angular spectra for excitation of the most important modes. The three different impact energies are representative of the three resonance regions. These data are extracted from a large number of energy loss spectra by taking the intensity value at the respective energy loss without any unfolding. Again, the Born dipole cross section is plotted with the IR-active modes $\nu_{1,4}$, ν_2 and ν_5.

A remarkable feature of the angular spectra is the cross section for the excitation of $\nu_{1,4}$ which is steeply increasing and quite close to the BDA in forward direction. This cross section can be regarded as the sum of a direct and a resonant component. The latter one, which is independent of the scattering angle within the error bars, predominates at higher angles. In the first resonance, $\nu_{1,4}$ is mainly excited via direct scattering

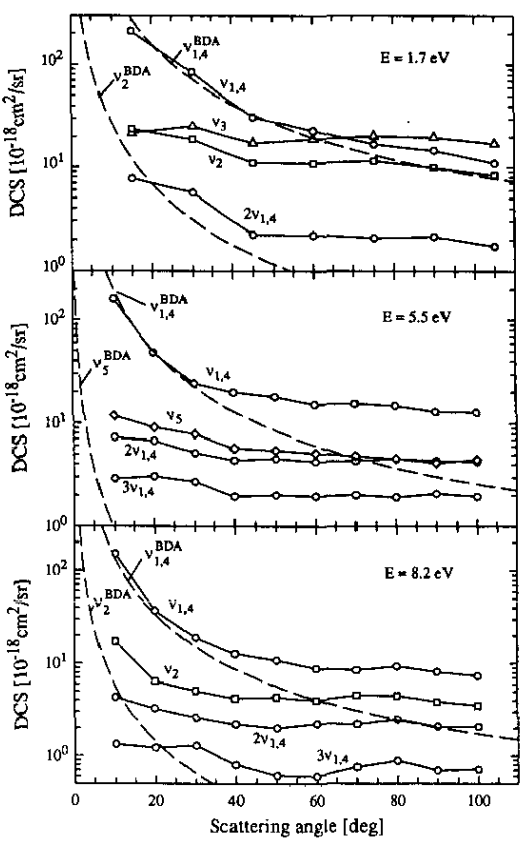

Figure 7. Angular spectra for the most important energy loss processes in e-CF_3Cl scattering. The collision energies are representative of the three resonance regions. The Born dipole cross sections for the excitation of $\nu_{1,4}$, ν_2, and ν_5 are indicated by dashed lines.

as already discussed before. The deviation from the (rather large) BDA is quite small even for the larger angles. In the (C–F σ^*) resonances, the point with about equal contributions from both mechanisms is reached at a scattering angle between 40° and 50°.

A similar interpretation, but with different proportions of direct and resonant excitation can be given for the other modes. As their IR activity is small or even negligible, the forward direction is less ($2\nu_{1,4}$, ν_2, ν_5) or not at all pronounced ($3\nu_{1,4}$, ν_3). At $E = 1.7$ eV, the ν_3 excitation governs the energy loss at large angles, but is much smaller than $\nu_{1,4}$ and about equal to ν_2 at $\vartheta = 15°$. All other depicted curves do not intersect, since the larger cross section for resonant scattering goes along with a larger cross section for direct scattering.

According to the theory of angular distributions for resonant scattering (Andrick and Read 1971, see also paper II), predominantly isotropic scattering is expected for the excitation schemes $A_1 \rightarrow A_1 \rightarrow A_1$ and $A_1 \rightarrow E \rightarrow E$ (the notation indicates the symmetry type of the ground vibrational state, the resonant state, and the final vibrational state, respectively). The first scheme is realized by the excitation of ν_2 and ν_3 in the 2.0 eV resonance and the excitation of ν_1 and ν_2 in the 8.5 eV resonance, whereas the second scheme describes the excitation of ν_4 and ν_5 in the 5.5 eV resonance. In all cases mentioned, the experimental findings are in accordance with the expected isotropic behaviour of the resonant excitation process.

A particular case is given for the excitation of ν_1 in the 5.5 eV resonance. According to the assignment given above, this excitation process corresponds to the scheme $A_1 \rightarrow E \rightarrow A_1$. If only the lowest possible partial wave ($p\pi$) is considered, the angular distribution would have the form $W(\vartheta) = 1 + 7\cos^2\vartheta$ which shows a pronounced minimum at $\vartheta = 90°$. No evidence for such a behaviour is found in the experimental results. An explanation may be sought in two ways, either the ν_1 excitation is present in the 5.5 eV resonance to a lesser amount than suggested by the energy loss spectra or the representation by a pure $p\pi$ wave is a too simple description of the E (C–F σ^*) resonance at 5.5 eV. In any case, an improvement of the experimental conditions towards a better resolution of the ν_1 and ν_4 excitations appears highly desirable to solve these questions.

Similar difficulties arise in the discussion of the angular distributions for the excitation of the higher harmonics and combination modes $2\nu_{1,4}$ and $3\nu_{1,4}$. The symmetry type of these modes is given by the (symmetric) product of the symmetry types of the normal modes involved and thus contains A_1 for $n\nu_1$, E for $(n-1)\nu_1 + \nu_4$, and both symmetry types for any mode with more than one quantum of ν_4 (the latter leads to doublets; see de Souza and Perry (1986) for more details). The experimental observation of a mostly flat angular distribution for these excitations, which would be favoured by the E symmetry of $(n-1)\nu_1 + \nu_4$, goes along with the findings from the energy loss spectra (see figure 5) that the centres of the peaks approximately correspond to the excitation of one quantum of ν_4. But again, it must be emphasized that a better experimental resolution is needed to clarify these questions.

4. Dissociative attachment and resonant vibrational excitation

Stable CF_3Cl^- ions have been found only in experiments with CF_3Cl clusters where the evaporation of monomers removes the excess energy (Kühn and Illenberger 1990). Under single collision conditions with the monomer, the temporary negative-ion state

is always decaying. Besides autodetachment of the electron leading to elastic scattering or vibrational excitation, the molecule can dissociate into two or more fragments with the electron staying with one of the fragments. The branching ratio is governed by the time scales of the decay processes in comparison with the nuclear motion induced by the attachment of the extra electron (see also discussion in paper II). Absolute cross sections for the negative-ion production in e-CF_3Cl scattering are given by McCorkle *et al* (1980) and, in more detailed form, by Spyrou and Christophorou (1985). Below 10 eV, essentially two maxima are found corresponding to the two lower σ^* resonances with a total attachment cross section of $\sim 10^{-18}$ cm^2. An estimate of the integral cross section for vibrational excitation (see figure 4 and figure 6) leads to a value of $\sim 5 \times 10^{-16}$ cm^2 in both resonances. This value is comparable with the resonant part of the total inelastic cross section as derived in figure 3. Similar to e-CF_4 scattering, it appears that the negative-ion decay via autodetachment is a fast process and that vibrational excitation is the dominating decay channel. Consequently, we expect a shift of the energetic positions of the resonances in dissociative attachment (DA) towards lower energies, whereas the excitation functions for vibrational excitation should reflect the primary shape and position of the resonances.

In table 3, a compilation of the DA results concerning the decay of the resonances is given. In the first resonance, only the Cl^- ion is produced in accordance with the (C-Cl σ^*) character. The corresponding vibration, the C-Cl stretching mode ν_3, is found to be strongly excited in this resonance with a rather large cross section. But also the resonant excitation of ν_2 and possibly $\nu_{1,4}$ is observed with a remarkable cross section. This may be attributed to the fact that the charge distribution of the (C-Cl σ^*) orbital reaches beyond the central C atom into the CF_3 part of the molecule and thus induces CF_3 deformation and stretching motions. In agreement with the discussion of the time scales given above, the maximum of the ion production peak is found at a lower energy than the value of 2.0 eV observed in vibrational excitation and in the total cross section (Jones 1986). The production of other negative ions is energetically forbidden due to their higher heats of formation (see table 3).

Table 3. Negative-ion production in e-CF_3Cl scattering. The values for the heat of reaction ΔH_0 are given following Spyrou and Christophorou (1985) (SC). The energetic positions of the maxima in the negative-ion yield curves and the corresponding relative intensities are taken from Illenberger (1982) and Spyrou and Christophorou (1985), respectively.

Ion	Neutral fragment(s)	ΔH_0 (eV)	Illenberger (1982)		SC (1985)	
			E (eV)	Rel. int.	E (eV)	Rel. int.
Cl^-	CF_3	0.1	1.3	0.5	1.4	1000
F^-	CF_2Cl	1.9	4.1	0.4	4.3	500
FCl^-	CF_2	3.0	3.9	0.4	4.7	10
CF_2Cl^-	F	3.6	4.2	0.2	4.4	75
Cl^-	CF_2+F(?)	4.1	4.8	1.5	5.0	550

Between 4 and 5 eV, several negative ions are observed which are most likely to be connected with the E (C-F σ^*) resonance at 5.5 eV. The electron capture into an antibonding C-F orbital is reflected in the production of F^- and CF_2Cl^-. But also Cl^- is found with a large intensity and without its counterpart CF_3^-. While the production

of F_2^- is not reported, FCl^- is observed, however the values of the relative intensities differ considerably. It may also be possible that some of these channels belong to the A_1 (C-F σ^*) resonance, but the energy difference to the presently derived value of $E = 8.5$ eV seems to be rather large. Illenberger (1982) found small peaks in the F^- and Cl^- production around 9 eV, but it is questionable if these processes correspond to electron capture into a valence orbital. We conclude that there seems to be no simple relation between the observed fragments and the properties of the (C-F σ^*) resonances. In contrast, the process of resonant vibrational excitation in this energy region follows a much simpler scheme. It shows a smaller number of exit channels with the dominant appearance of the C-F stretching modes $\nu_{1,4}$ and a contribution of either the symmetric (ν_2) or the asymmetric (ν_5) CF_3 deformation mode. These vibrations clearly reflect the character and the symmetry of the resonances.

5. Conclusions

Electron capture processes in low-energy e-CF_3Cl scattering are known from electron transmission (e.g. Jones 1986) and dissociative attachment experiments (e.g. Illenberger 1982, Spyrou and Christophorou 1985). Together with the present results on vibrationally elastic and inelastic scattering, a quite detailed description of the interaction of low-energy electrons with CF_3Cl molecules can be achieved. It has been shown in the present paper that state-resolved measurements of the vibrational excitation channels, in combination with the selection rules as originally formulated by Wong and Schulz (1975), provide detailed information on the resonant states which goes beyond the possibilities of the other experimental methods. The difficulties due to the existence of six normal modes and the quickly growing density of combination modes appears at first sight to overcharge the possibilities of a crossed-beam electron scattering experiment with its limited energy resolution, but the selection mechanisms account for quite simple excitation schemes, thus rendering possible detailed studies in spite of the complexity of the molecule.

Comparing e-CF_3Cl with e-CF_4 scattering (see paper II), several differences are noticeable. Probably due to the permanent dipole moment of CF_3Cl, the Ramsauer-Townsend minimum in the elastic cross section is less pronounced. The elastic cross section is generally larger by nearly a factor of two. The non-resonant vibrational excitation of both molecules is described in a similar way by the Born dipole approximation. New aspects, however, appear in the resonant excitation process due to the possibility of both (C-F σ^*) and (C-Cl σ^*) type resonances. The A_1 (C-Cl σ^*) resonance is located at 2.0 eV. The dominant excitation is the symmetric C-Cl stretching mode ν_3, but also CF_3 deformation (ν_2) and stretching ($\nu_{1,4}$) modes are excited in this resonance. The E (C-F σ^*) and A_1 (C-F σ^*) resonances are assigned for the first time to be located at 5.5 eV and 8.5 eV, respectively. The predominant excitation of the CF_3 stretching modes $\nu_{1,4}$ is accompanied by the excitation of the CF_3 asymmetric deformation mode ν_5 in the first case and the CF_3 symmetric deformation mode ν_2 in the second case, both in accordance with the symmetry type of the respective resonance.

A clear relation with dissociative attachment exists in the case of the A_1 (C-Cl σ^*) resonance, whereas the fragmentation behaviour in the region of the (C-F σ^*) resonances appears to be more complex. A detailed knowledge of the CF_3Cl^- potential surfaces is probably necessary to understand all features of the decay processes of the resonant states.

References

Andrick D and Read F H 1971 *J. Phys. B: At. Mol. Phys.* **4** 389-96
Bishop D M and Cheung L M 1982 *J. Phys. Chem. Ref. Data* **11** 119-33
Christophorou L G and Hunter S R 1984 *Electron-Molecule Interactions and their Applications* vol II, ed L G Christophorou (Orlando: Academic) pp 317-422
de Souza A M and Perry D S 1986 *J. Phys. Chem.* **90** 4508-13
Herzberg G 1945 *Molecular Spectra and Molecular Structure, Part II: Infrared and Raman Spectra of Polyatomic Molecules* (New York: Van Nostrand Reinhold)
Illenberger E 1982 *Ber. Bunsenges. Phys. Chem.* **86** 252-61
Itikawa Y 1971 *J. Phys. Soc. Japan* **30** 835-42
—— 1974a *J. Phys. Soc. Japan* **36** 1121-6
—— 1974b *J. Phys. Soc. Japan* **36** 1127-32
Jones R K 1986 *J. Chem. Phys.* **84** 813-9
Jordan K D and Burrow P D 1987 *Chem. Rev.* **87** 557-88
Kühn A and Illenberger E 1990 *J. Chem. Phys.* **93** 357-64
Mann A and Linder F 1992a *J. Phys. B: At. Mol. Opt. Phys.* **25** 533-43
—— 1992b *J. Phys. B: At. Mol. Opt. Phys.* **25** 545-56
McCorkle D L, Christodoulides A A, Christophorou L G and Szamrej I 1980 *J. Chem. Phys.* **72** 4049-57
Scanlon K, Suzuki I and Overend J 1981 *J. Chem. Phys.* **74** 3735-44
Schumacher R, Sprunken H-R, Christodoulides A A and Schindler R N 1978 *J. Phys. Chem.* **82** 2248-52
Spyrou S M and Christophorou L G 1985 *J. Chem. Phys.* **82** 2620-9
Sverdlov L M, Kovner M A and Krainov E P 1974 *Vibrational Spectra of Polyatomic Molecules* (New York: Wiley)
Verhaart G J, van der Hart W J and Brongersma H H 1978 *Chem. Phys.* **34** 161-7
Wong S F and Schulz G J 1975 *Phys. Rev. Lett.* **35** 1429-32